

A pH plate fluorosensor (optode) for early diagenetic studies of marine sediments

Stefan Hulth

Department of Analytical and Marine Chemistry, Göteborg University, SE-412 96 Göteborg, Sweden

Robert C. Aller

Marine Sciences Research Center, SUNY at Stony Brook, Stony Brook, New York 11794-5000

Pia Engström and Erik Selander

Department of Analytical and Marine Chemistry, Göteborg University, SE-412 96 Göteborg, Sweden

Abstract

Pore water pH distributions are closely coupled to early diagenetic reactions and transport processes in surficial sediments. In this study, an optical plate fluorosensor for rapid two-dimensional detection of H⁺ concentration patterns in sediment pore waters was developed. The dual excitation (405/450 nm) single emission (520 nm) pH fluorophore HPTS (8-hydroxypyrene 1, 3, 6, trisulfonic acid trisodium salt) was immobilized onto transparent, supporting sensor foils. Excitation/emission spectra of immobilized HPTS exhibited pH dependent shifts in seawater standards, and fluorescence excitation ratios were used for two-wavelength, ratiometric detection of pH distributions in sediment and bottom water close to the sediment–water interface (pH ≈ 6.5 to 8.5). Sensor foils were fixed to the inner sides of plastic box corers or glass plate aquaria containing sediment and overlying seawater. Equilibration with pore water occurred in seconds, and fluorescence response (excitation/emission) was scanned nondestructively using a monochrome, integrating CCD camera. The two-dimensional sensor system has a vertical and horizontal resolution of 56 × 54 μm (5 × 5 pixels) applied over an image of 34 × 26 mm. Reproducibility and accuracy were best when foils were prepared from solutions of similar ionic strength to samples. Optical sensor pH distributions correlated well with high-resolution, vertical distributions measured simultaneously with a minicombination pH electrode, and two-dimensional pH patterns demonstrated directly the transport–reaction heterogeneity associated with microtopography and biogenic structures in surface deposits and overlying waters close to the sediment–water interface. Sensor foils retained calibration characteristics for at least 50 d.

The activity of hydrogen ions (pH) is a master geochemical parameter reflecting the thermodynamic state of acid-base processes and overall balances between multiple reaction and transport processes within natural environments (e.g., Sørensen and Palitzsch 1910; Takahashi et al. 1970; Dickson 1993). Surficial marine sediments, in particular, are characterized by complex heterogeneity and steep gradients in reaction rates, concentration distributions, and mass transport efficiency (Revsbech et al. 1980; Reimers et al. 1986; Revsbech 1989; Glud et al. 1996; Aller et al. 1998). Measurements of pH in surficial sedimentary deposits are typically made using H⁺ sensitive glass electrodes (e.g., Revsbech and Jørgensen 1986; Cai and Reimers 1993). Although pH electrodes are ideal for many applications, they are limited in resolving spatial patterns, are subject to matrix-related standardization uncertainties (e.g., liquid junction potential and solution interferences—poisoning), may suffer from electrical interferences and physical damage, and are in some formats relatively expensive (Sillén 1967; Revsbech 1989; Wolfbeis 1991). Spectrophotometric pH measurements offer an alternative to potentiometric techniques (Byrne and Breland 1989; Dickson 1993; Lakowicz 1999), and optical sen-

sors are in principle well-suited for resolving both micro and macro spatial distributions in sedimentary environments. Optical sensors are usually simpler and less expensive to construct than electrodes, can be used in remote detection schemes, and normally have superior long-term stability (Wolfbeis 1991; Klimant et al. 1995; Lakowicz 1999; Strömberg and Hulth 2001). In the present study, we developed and investigated the use of a planar optical pH sensor, specifically designed for resolving high-resolution, two-dimensional pH distributions in surface sediments. The pH plate fluorosensor has the potential to greatly improve understanding of mineralization and general reaction processes during early diagenesis in surficial sediments.

Over the past two decades, considerable effort has been directed toward the development of solute specific chemical sensors with optical detection (e.g., Harvey 1957; Peterson et al. 1980; Seitz 1984; Lakowicz 1999). These optical sensors are often called optodes (derived from *οπτοδεδε*—the optical way) or optrodes (in analogy to the term electrode). The first fiber optic pH sensor was developed for *in vivo* studies by Peterson et al. (1980) and related pH to the absorbance of immobilized phenol red (phenolsolphthalein). Owing to the general importance of pH measurements, a large number of pH optodes have been designed (e.g., Saari and Seitz 1982; Zhujun and Seitz 1984; Offenbacher et al. 1986; Wolfbeis and Offenbacher 1986; Leiner and Wolfbeis 1991). They all, however, rely on luminescence properties of the acid/base conjugate pair of the pH indicator. A wide

Acknowledgements

Financial support was obtained from the Swedish Natural Science Research Council (NFR) and the National Science Foundation (NSF OCE9730933). N. Strömberg and J. Arvidsson provided technical and laboratory assistance. We thank R. Glud and an anonymous reviewer for comments on the manuscript.

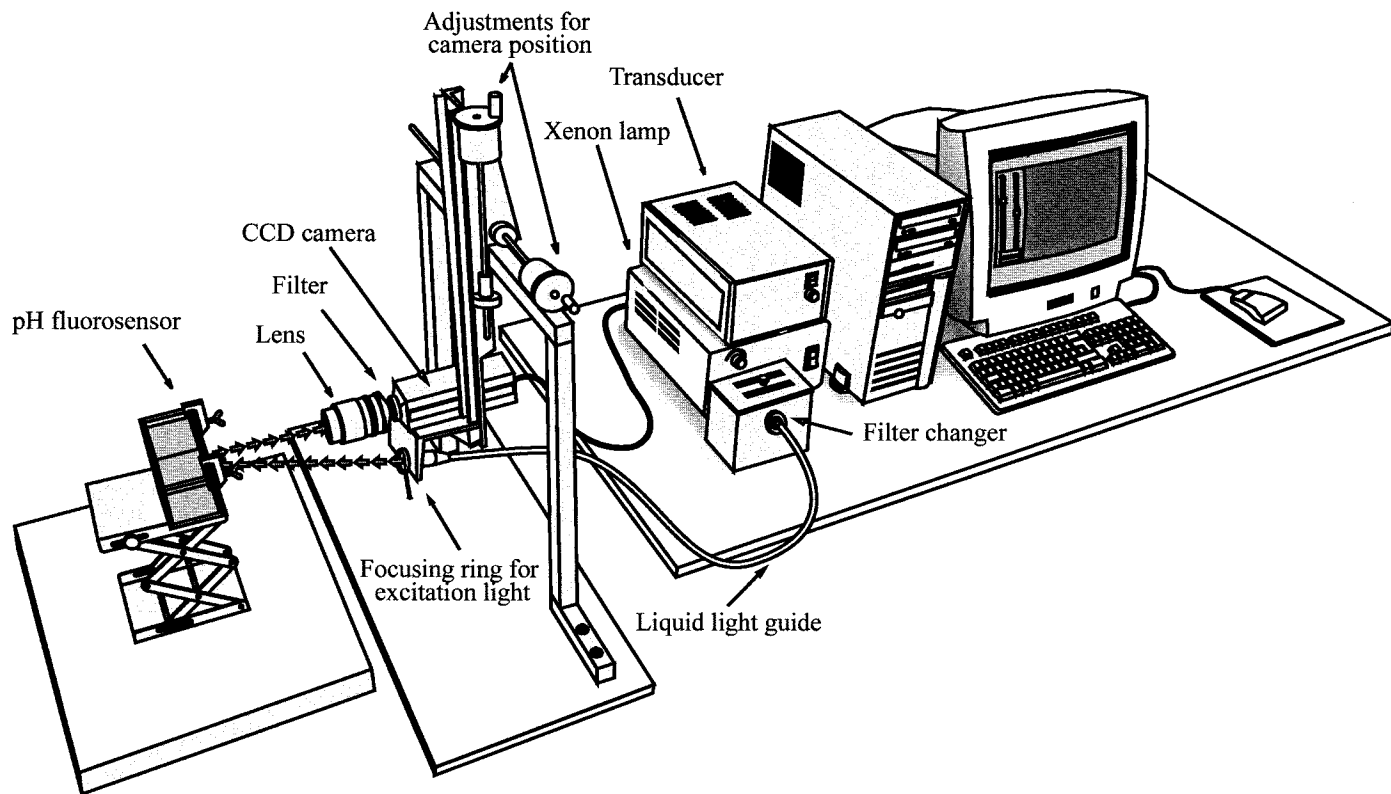


Fig. 1. Optical system used for two-dimensional quantification of pH distribution patterns in aquatic sediments. The setup is a custom-made adaptation of an optical imaging and photometry system originally designed for two-wavelength ratiometric detection of in vivo calcium concentrations.

range of fluorescent indicators of O_2 , CO_2 , Ca^{2+} , and pH have been used in the development of gas and ion-specific fiber optic sensors in medical and health sciences (e.g., Peterson et al. 1980; Grynkiewicz et al. 1985; Wolfbeis 1985). However, it was not until recently the technique was introduced to aquatic biogeochemistry by a microfluorosensor for oxygen (Klimant et al. 1995; Glud et al. 1999a).

Planar optodes, or plate fluorosensors, are similar to fiber optodes but the solute specific fluorochrome is immobilized and imaged on a foil sheet instead of a small fiber tip (Glud et al. 1996). Planar optodes using a Ru-fluorophore have been used for the detection of two-dimensional oxygen distribution patterns in surface sediments and in high-resolution studies of early diagenetic processes and oxygen dynamics in photosynthetic microbial mats and bacterial biofilms (Glud et al. 1996, 1998, 1999). In principle, planar sensor foils of various types can be fixed onto transparent plates and inserted or otherwise brought into contact with sediment. After equilibration with sediment pore water, the indicator can be optically scanned (excitation and emission) nondestructively through the transparent plate to obtain a two-dimensional "picture" of solute distributions. Photometric detection of fluorescence from plate sensors can either be done in the laboratory subsequent to removing the sensor from the sediment or directly in situ using more sophisticated benthic lander technology (Smith et al. 1976; Rhoads and Germano 1982; Nilsson and Rosenberg 2000). One such benthic camera system (Hyperspectral REMOTS) is pres-

ently equipped for UV excitation/emission scans for detection of autofluorescent anthropogenic contaminants (pyrenes), but has not yet been used to determine specific solute distributions in situ (Rhoads et al. 1994).

Materials and Methods

Two-dimensional optical system—The optical system used in this study is a custom adaptation of the InCyt Pm2[®] imaging and photometry system (Intracellular Imaging), originally designed for ratiometric fluorophore studies of individual cells. In this modified version, a liquid light guide transferred excitation light to the sample (Fig. 1). Light emitted by the plate fluorosensor was collected by an eight-bit COHU 4910 integrating monochrome CCD camera (chip resolution 753×582 pixels). The theoretical individual pixel resolution for the COHU camera as set up was $8.5 \times 8.2 \mu\text{m}$. NIKON standard single lens reflex (SLR) lenses were used to optimize spatial resolution and size of the image. Effective image resolution was $56 \times 54 \mu\text{m}$ at the distance employed between plate sensor and camera (20–40 cm). The system also included a 300 W Xe UV/VIS arc lamp, a computer controlled dual filter changer (405/450 nm) at the excitation side, and an emission filter (520 nm) mounted between the lens and camera (Fig. 1). The data acquisition/analysis software InCytIm2[®] was controlled by a Windows-based PII-400 MHz computer. Bitmap images were evaluated by taking the ratio of fluorescence intensity

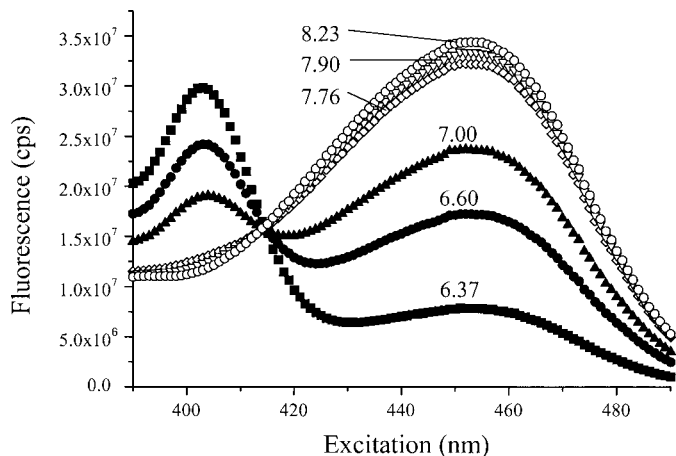


Fig. 2. Excitation spectra of HPTS dissolved in seawater (salinity of 32) at different pH values. HPTS is a dual excitation (405/450 nm)–single emission (520 nm) fluorochrome with pH dependent excitation and emission maxima.

(excitation 405/450 nm; emission 520 nm) in each pixel using the geographical information system (GIS) software program IDRISI[™] (version I32.11; ClarkLabs). After pixel ratioing and pH calibration, 5 × 5 adjacent pixels regions were Gauss filtered to reduce noise. Owing to the properties of Gauss filtering, final image resolution remained at 56 × 54 μm.

When pH values obtained using the plate fluorosensor were compared with profiles obtained with a minicombination pH electrode, fluorosensor values at corresponding profile depths were taken as the average within discrete 1 × 60 mm (vertical × horizontal) layers and assigned to the depth interval midpoints. Replicate fluorosensor distributions were recorded by horizontally adjusting the camera position 2–3 cm, while electrode distributions were recorded approximately 1 cm apart.

HPTS—A number of fluorescent pH indicators are known, but relatively few meet the requirements of excitation/emission in the visible spectrum. A visible response region allows the use of inexpensive optics and light guides, as well as inexpensive light sources such as halogen lamps. In addition, a large Stokes' shift is advantageous to separate incident excitation from emission. Further desired requirements are photostability, lack of toxicity, and presence of functional groups suitable for immobilization onto supports (Wolfbeis 1991).

HPTS (8-hydroxypyrene 1, 3, 6, trisulfonic acid trisodium salt) is one of the most widely used fluorescence pH indicators (e.g., Wolfbeis et al. 1983; Wolfbeis 1985). HPTS is a weak organic acid that has different fluorescence spectra in the dissociated (deprotonated) and associated (protonated) form. It is a dual excitation (405 and 450 nm) single emission (520 nm) fluorochrome with ratiometric properties (Fig. 2). Visible excitation/emission response allows the use of less expensive optical setups. A pK_a value close to neutral (Wolfbeis et al. 1983) makes it almost ideal for pH studies in cells and living materials, as sensor dynamic range normally covers a pH range of $pK_a \pm 1$ pH unit (Bishop 1972).

HPTS trisodium salt is known to have excellent water solubility, have a quantum yield close to 1, lack toxicity, and hold appropriate functional chemical groups (sulfonate) suitable for covalent immobilization onto, for example, cellulose acetate. Lack of toxicity makes it advantageous to use plate fluorosensors in the sediment also for extended time periods (weeks to months).

Preparation of sensing foil—The optical pH-sensitive foil contains a two layer polymeric support onto which the pH fluorochrome HPTS was immobilized. A prefabricated, transparent plotter foil (Hewlett Packard, HP C3835A) made from a 100-μm polyester layer covered on one side with a 10-μm layer of cellulose acetate was found appropriate for HPTS immobilization. Cellulose and cellulose acetate are polymeric supports well-suited for immobilizing solute specific indicators. They can be optically transparent and have good permeability for ions, including protons (e.g., Kostov et al. 1993; Werner and Wolfbeis 1993). Various pH indicators can be either covalently incorporated (Kostov et al. 1993) or physically entrapped by hydrophobic interactions into these supports (Cardwell et al. 1993). In this study, the fluorochrome HPTS was linked to the cellulose acetate simply by immersing the OH foil overnight into a solution of 4 μM HPTS. The HPTS solution was made up from filtered (0.3 μm) seawater or artificial seawater (Hansson 1973) diluted to appropriate salinity using Milli-Q water. New sensor foils were rinsed in filtered (0.3 μm) seawater for at least 24 h. Prior to use, foils were additionally soaked in a solution of ionic strength corresponding to that of samples. Although the exact mechanism of dye incorporation and nature of interactions between sensor foil and HPTS are not yet fully understood, our data indicate that high ionic strength and pH above neutral result in irreversible HPTS immobilization. Sensor foils were transparent after immobilization, and sampled sediment and sediment structures could therefore be visually inspected as well as photometrically analyzed using the CCD camera and the IDRISI[™] software. Although transparent sensor membranes may seem advantageous, fluorescence response from such membranes also includes interactions normally associated with the physical structure of the sediment matrix (e.g., light scattering from sand grains and absorption of light in burrows and holes). Part of this drawback can be compensated for by subtracting background images from obtained fluorescence patterns. Background fluorescence from sensor foils was found insignificant.

Sensor calibration and pH pore water distributions—In order to increase reproducibility and accuracy of pH measurements in marine environments, an alternative convention has been proposed to define pH standards in terms of their total H^+ concentrations in seawater (Dyrssen and Sillén 1967; Sillén 1967; Hansson 1973). On this ionic medium scale (as opposed to infinite dilution), the activity coefficients are dominated by the bulk electrolyte and therefore become unity as the solution approaches the pure ionic medium. No extrapolation or extrathermodynamic assumptions are generally necessary for pH determinations on the ionic medium scale in marine systems. Therefore, foils were pre-

pared, handled, and standardized in solution matrices similar to those of the target samples. Buffers were solutions prepared in synthetic seawater as described by Hansson (1973). Fluorosensor response was compared with microcombination glass pH electrodes with Ag/AgCl reference (Micro-electrodes), also calibrated according to the ionic medium standard state (Dyrssen and Sillén 1967; Hansson 1973; Dickson 1990). During standardization, the sensor foil was attached to one side of a specially designed glass aquarium ($20 \times 8 \times 8$ cm) containing ordinary seawater (salinity 32; alkalinity $2250 \mu\text{M}$) of different pH values simultaneously monitored with the electrode. Working standards for pH were achieved by the addition of 10 mM HCl or 0.1 M NaOH, diluted with NaCl of appropriate concentration to match sample ionic strength.

Sediment subsamples (the Gullmars Fjord, western Sweden) were taken from boxcores (25×25 cm) by gently inserting a specially designed 15×15 cm Plexiglas container into the sediment. The container was open at both ends. Prior to insertion, all four sides of the container were covered with ready-to-use pH fluorosensor foils. Sensors were protected from light to minimize eventual photobleaching of the indicator. Subsequent to subsampling, the container filled with water and sediment was transferred to the laboratory for photometric analysis using the optical setup (Fig. 1). In between sampling and fluorescence detection, overlying water was aerated and the container kept at in situ temperature.

In addition to detection of two-dimensional distributions in intact sediment cores, surface (0–2 cm) sediment was removed, sieved (1 mm), and homogenized for quantification of pH distributions in reactive surface sediments. The sediment was carefully transferred to a glass aquarium ($30 \times 30 \times 25$ cm), after which bottom water from the sampling site was added. Care was taken to keep the sediment–water system in the dark and maintain overlying water aerated. During actual photometric analysis there was no aeration or stirring of the overlying water. Two-dimensional pH distribution patterns were also observed in a microcosm containing initially homogenized surface (0–2 cm) sediment from Flax Pond (Long Island Sound, USA) using a comparable optical system with a peltier cooled 14 bit camera.

Results and discussion

Sensing foil synthesis and properties—One of the most common problems with optical sensors, besides photobleaching of the indicator, is related to the binding stability and association of fluorophores with the carrier (Wolfbeis 1991). Indicator immobilization can in fact largely determine characteristics and performance of the sensor (Lin 2000). HPTS has previously been immobilized electrostatically on anion exchange membranes (Zhujun and Seitz 1984) and covalently bound to glass and cellulose (Offenbacher et al. 1986; Kostov et al. 1993). Although the indicator layer in some of these sensors was found not stable to strong bases or acids, covalent binding is normally quite reliable, and the indicator does not significantly leach out from sensor membranes.

Membrane preparation as developed in this investigation was simple and effective; however, certain conditions were found necessary for optimal performance. For example, excessive concentration of HPTS on sensor foils can promote inner-filter effects (Lakowicz 1999), alter apparent pK_a (Wolfbeis 1991), and promote desorption during deployment. Sensor membranes were in this study therefore prepared from solutions of $4 \mu\text{M}$ HPTS. Using this procedure, there were no signs of inner-filter effects or dye leaching from sensor foils once treated with HPTS and soaked in seawater (data not shown). Observed maximal change in fluorescence ratio for the HPTS concentrations tested (0– $25 \mu\text{M}$) corresponds to a pH shift of less than 0.1 pH unit.

It is important to note that although incorporation of HPTS on the foil may not be exactly uniform, the use of ratiometric wavelength detection largely eliminates concentration dependent effects within a foil over the immobilization range used and minimizes any variation in response between foils (e.g., Leiner and Wolfbeis 1991). It was beyond the scope of the present study to investigate the complex nature of interactions between sensor foil and HPTS or its exact concentration distribution on the foil surface.

Stability of optical sensors is normally excellent (Wolfbeis 1991; Klimant et al. 1995), as was also the case for the HPTS pH fluorosensor. After extended periods, HPTS sensor membranes showed no significant change in calibration (data not shown). Sensors inserted into the sediment for more than 50 d still retained fluorescence characteristics, and one-point calibrations performed in the overlying water confirmed that sensors could be used for detection of two-dimensional pH distributions in sediments also after extended periods of deployment. This stability implies that HPTS pH fluorosensors can be used during sediment monitoring, although artifacts associated with, e.g., biofouling may become a problem. Observed long-term stability further suggests that the HPTS membranes are resistant to alteration by diagenetically produced solutes such as HS^- and Fe^{2+} .

Owing to the thin reactive cellulose acetate layer, the acid-base equilibrium of the pH indicator is established within seconds. Sensor response time was estimated to be less than 5 s. Response time of a plate fluorosensor should be dependent on stirring of surrounding water and existence of a diffusive layer covering the sensor surface. It is assumed that thin membranes and efficient mixing give the shortest sensor response times, but no detailed evaluation of these factors was made.

HPTS pH fluorescence response—HPTS immobilized on the cellulose acetate–polyester support did not change basic spectral properties compared to HPTS in free solution (Figs. 2 and 3). Immobilized HPTS retained both its Stokes' shift and general excitation/emission response as a function of pH. Maximum excitation was slightly shifted to longer wavelengths, and fluorescence at 405 nm increased relative to 450 nm for immobilized HPTS. However, these changes did not significantly affect overall sensor response to sample pH. The ratio of excitation at 405 and 450 nm (emission 520 nm) was a sensitive but nonlinear measure of pH, with a sigmoidal change of fluorescence ratio with increasing sample pH reflecting the titration of immobilized HPTS (Fig.

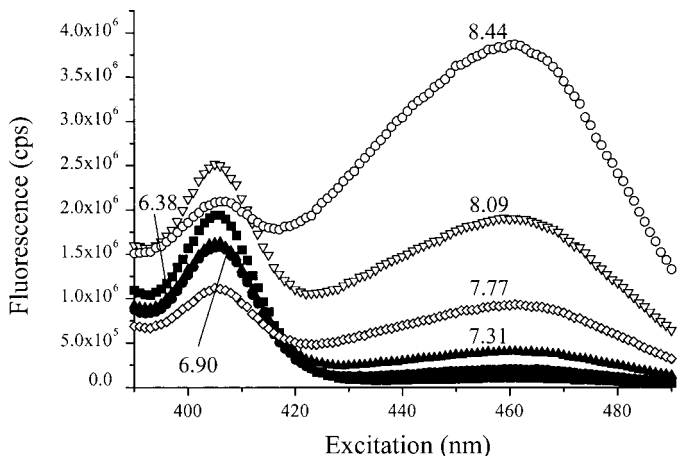


Fig. 3. Excitation spectra of HPTS immobilized on the sensor foil immersed in seawater at different pH values. Compared to HPTS dissolved in seawater, excitation maxima for the pH plate fluorosensor were slightly shifted to longer wavelengths and fluorescence intensity at 405 nm favored compared to 450 nm.

4A). The inflection point is determined by the dissociation constant of the indicator, with the most sensitive response of the fluorosensor at a pH close to the apparent pK'_a (pK'_a) of the immobilized indicator. These response patterns were retained in the presence of common pore water constituents (NH_4^+ , Fe^{2+} , Mn^{2+} , HS^-) as demonstrated by standardization experiments in both oxic and anoxic pore water of varied composition (data not shown).

Sensitivity and effects of ionic strength—One important consideration of optical pH measurements is that concentrations of an indicator dye in either its acid or base form are determined rather than concentrations of H^+ directly. Relative spectral absorbance or fluorescence of the indicator dye

conjugate pair ($\text{H-Ind}/\text{Ind}^-$) is governed by the dissociation constant (K_a) of the organic molecule and pH of the sample. K_a is defined from the acid/base equilibrium:



$$K_a = \frac{\{\text{Ind}^-\}\{\text{H}_3\text{O}^+\}}{\{\text{H-Ind}\}\{\text{H}_2\text{O}\}} = \frac{\gamma_{\text{T,Ind}^-}\gamma_{\text{T,H}_3\text{O}^+}[\text{Ind}^-][\text{H}_3\text{O}^+]}{\gamma_{\text{T,H-Ind}}[\text{H-Ind}]} \quad (2)$$

Rearranging Eq. 2 gives the Hendersson-Hasselbach equation

$$\text{pH} = pK_a + \log \frac{[\text{Ind}^-]}{[\text{H-Ind}]} + \log \frac{\gamma_{\text{T,Ind}^-}\gamma_{\text{T,H}_3\text{O}^+}}{\gamma_{\text{T,H-Ind}}} \quad (3)$$

where $\{X_i\}$ is the activity of component i , $[X_i]$ is the total concentration of i , and $\gamma_{T,i}$ the solute total activity coefficient of ion X_i in solution (or $\lambda_{T,i}$ on the solid surface).

It is clear from Eq. 3 that changes in ionic strength and solution composition will produce changes in indicator speciation and thus influence fluorescence response as a function of pH. Total activity coefficients depend on both non-specific (ionic strength) and more specific interactions such as complex formation (e.g., Stumm and Morgan 1996). Decreases in activity coefficients, particularly of charged species, due to nonspecific interactions with increased ionic strength should shift the ratiometric response curve of Fig. 4A to a lower pH range (Kostov et al. 1993). In the present case, seawater with a total ionic strength of about 0.6 mM indeed caused a negative shift in apparent pK'_a compared to a buffer solution ($I_{\text{tot}} \approx 0.1$ mM; Fig. 4B). Eventual loss of free Ind^- from sensor surface or a change in fluorescence behavior of either indicator species would superimpose effects caused by increasing ionic strength.

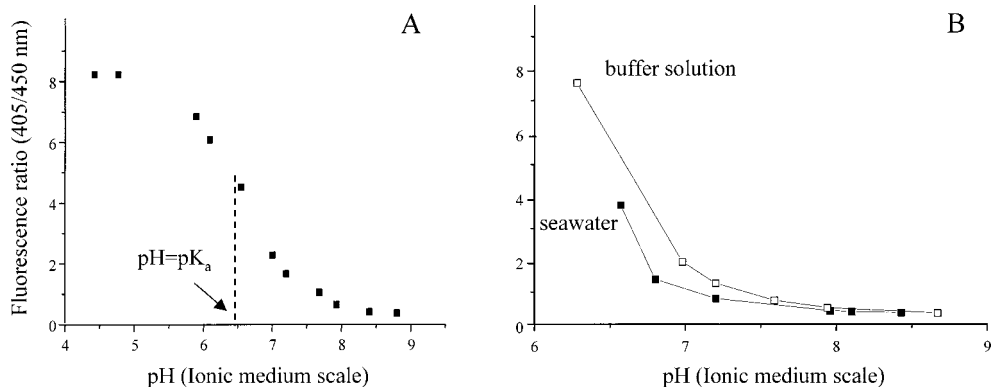


Fig. 4. (A) Fluorescence ratio 405 nm over 450 nm (emission 520 nm) as a function of pH in seawater (salinity 32 and alkalinity 2250 μM). The pH electrode used for standardization was calibrated according to the ionic medium scale (Hansson 1973). At high pH values, HPTS is mainly in the dissociated form (Ind^-), while at low pH it is mainly in the associated (H-Ind) form. From the pH dependence, an apparent dissociation constant of approximately $10^{-6.4}$ (i.e., $pK'_a = 6.4$) could be calculated for HPTS immobilized onto cellulose acetate. (B) Sensor response was highly dependent on ionic strength of the sample, and the seawater caused a negative shift in apparent pK'_a compared to a buffer solution ($I_{\text{tot}} \approx 0.1$ mM). Total ionic strength was kept constant within the two treatments during the experiment.

Sensor response and apparent pK'_a of immobilized HPTS—Apparent (or effective) pK'_a of an immobilized indicator (pK'_a) is a primary factor to consider when identifying a suitable indicator for a particular application. The dissociation constant of an immobilized indicator can be quite different from that thermodynamically predicted, depending, e.g., on physical and chemical properties of the surface and the solution–surface interface (e.g., Bates 1973; Figs. 2, 3, and 4). The responses of pH optodes based on conventional pH indicators immobilized on sensor surfaces were thoroughly elucidated by Janata (1987). Overall errors in pH determinations were found mainly associated with changes in ionic strength of the solution. Ionic strength influenced both the solute activity coefficient of the indicator as well as the surface potential. The surface itself partially determines local acid-base properties and surface pH.

Normal response of an optical pH sensor with increasing pH corresponds to the titration of the immobilized dye, with a classical sigmoidal calibration having an inflection at the pK'_a of the immobilized indicator. The sensitivity of the sensor is most pronounced close to this pK'_a , where the derivative ($\delta(\text{signal})/\delta(\text{pH})$) is maximized. For the plate flurosensor, an apparent dissociation constant of $10^{-6.4}$ (i.e., $pK'_a = 6.4$) was observed for HPTS immobilized onto cellulose acetate (Fig. 4A). The dependence between the associated and dissociated form of the indicator, and limits inherent to instrumentation, set the dynamic range of optical and electrochemical pH sensors. For colorimetry and a two-color indicator, one color has been considered undetectable in the presence of the other when relative color intensity is less than one-tenth (Bishop 1972). These traditional limits fix optical sensor dynamic range to $pK'_a \pm 1$ pH unit.

Given a dynamic range of approximately $pK'_a \pm 1$ pH unit, the HPTS plate flurosensor should be most accurate for $5.4 \leq \text{pH} \leq 7.4$. This range is somewhat lower than the pH range often found in marine systems (Figs. 5 and 6), but can be significantly extended if signal processing allows accurate detection of low concentrations of indicator species. For example, sensor dynamic range would cover 4 pH units ($pK'_a \pm 2$ pH units) if either of the two species in the indicator acid/base conjugate pair could be measured at a relative concentration of 1%. We found that extrapolation to pH above 7.5 is possible with our system, although uncertainty increases gradually at increasing pH due to reduced signal to noise ratios. For example, at pH 7.5 the emission ratio (405/450 nm) was 0.9 ± 0.1 , while at pH 8.0 this ratio was 0.4 ± 0.1 (Fig. 4A). The good correlation between pore water pH obtained using more conventional pH electrodes and pH detected using the plate flurosensor further indicated that the HPTS flurosensor also could be used for fine resolution measurements of pH distribution patterns at values commonly found in marine environments (Figs. 5 and 6).

Two-dimensional pore water distribution patterns of pH—Owing to a range of proteolytic and hydrolytic reactions during early diagenesis, there is normally a sharp drop in pH at and just below the sediment water interface. In addition to a well-established pH gradient between overlying water and sediment, there is also typically a pH minimum at the sub-surface oxic/anoxic boundary, related in large part to reox-

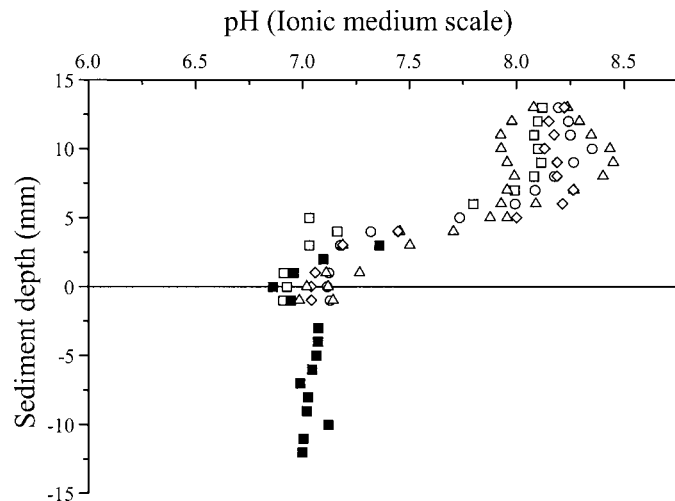


Fig. 5. Pore water distributions of pH in homogenized surface (0–2) sediments measured with the pH plate flurosensor (open symbols) and a minicombination pH glass electrode (filled squares) (measured on seawater ionic medium scale). When comparing pH in the Gullmar Fjord sediment, flurosensor point values at a certain sediment depth were evaluated as the average distribution within a 1×60 mm (vertical \times horizontal) layer of the sediment.

idation of reduced compounds diffusing from below (Revsbech et al. 1980). In the present experiments, vertical distribution patterns of pH consistent with these expectations were observed for both a minicombination pH electrode and the plate flurosensor in homogenized surface sediment from Long Island Sound and the Gullmar Fjord (Figs. 5 and 6). Five vertical recordings of pH distributions using the plate sensor were spread about 0.5 pH units in the overlying water from the Gullmar Fjord (Fig. 5). The relatively large discrepancy between pseudoreplicates may be caused by overlying water pH (7.9–8.5) approaching the limit for optimal range of the sensor. Also, small-scale heterogeneity was probably enhanced in the overlying water due to a lack of stirring or aeration during analysis. Stagnant conditions may have promoted the formation of concentration gradients in the water and in surficial sediment layers. The expected pH minimum just below the sediment water interface, along with progressively more constant pH conditions with depth in the sediment, were evident both in Gullmar Fjord and Long Island Sound sediments (Figs. 5 and 6). Below the oxic/anoxic boundary, differences between different plate sensor recordings were quite small, as was the pH difference relative the electrode. A relatively small difference between pore water replicate readings was expected as the sediment was initially homogenized and animals larger than 1 mm were removed. Below the surface redox boundary, sediment was anoxic and more or less independent of oxygen conditions in the overlying water.

Burrows, tubes, and fecal structures formed by benthic fauna superimpose various microenvironmental patterns of mineralization pathways onto the more traditional stratified reaction sequence (e.g., Froelich et al. 1979; Aller 1982; Aller and Aller 1998; Aller et al. 1998). Examples of small-scale heterogeneity and microniches associated with reactive organic material and locally enhanced mineralization of or-

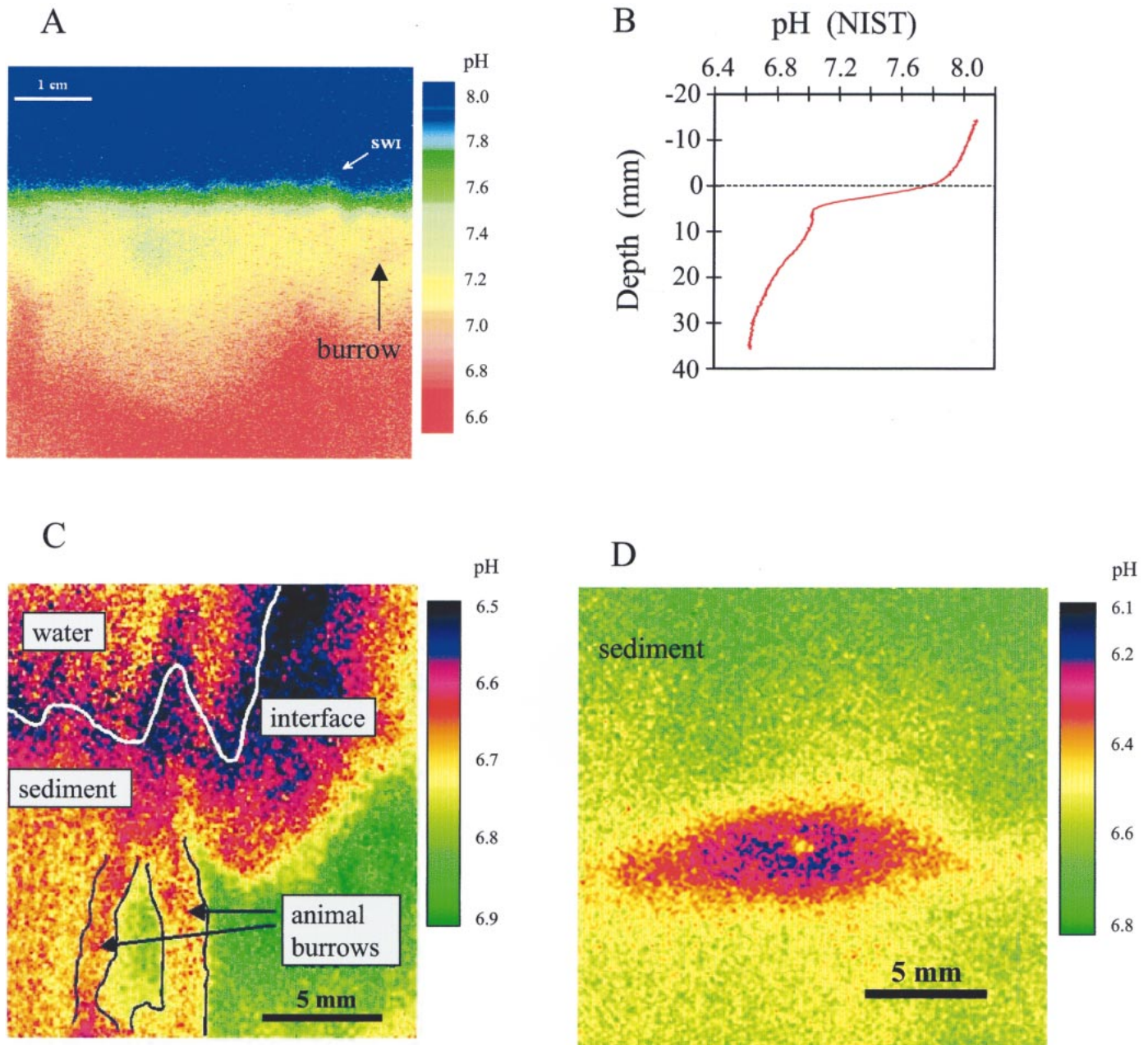


Fig. 6. (A) Example of two-dimensional pH distribution patterns in a sediment microcosm (from Long Island Sound) as elucidated by the HPTS fluorosensor. The plate fluorosensor pH values compared well with electrode readings (Ag/AgCl) from the same collection site (not shown). Both sensor types were in this example standardized on the NIST scale (infinite dilution). (B) The vertical profile plotted in this case represents the calculated one-dimensional average of the measured two-dimensional pattern (horizontally averaged across ~ 4.5 cm at each pixel depth). There was a sharp drop in pH at and just below the sediment water interface due to acid production during early diagenesis of organic matter. In addition to the strong pH gradient between overlying water and sediment, there was also a pronounced pH minimum at the subsurface oxic/anoxic boundary. A small U-shaped burrow is present in the upper right-hand side of the figure (A), the wall of which has a lower pH than ambient sediment. Such minima are in large part related to reoxidation of reduced compounds diffusing from below and oxidation of solid phase sulfides. Lateral deepening, shoaling, and expansion of iso-pH contours can be readily seen. This image has not been filtered in any way. (C) and (D) Examples of two-dimensional pore water distribution patterns of pH in intact sediment cores detected using the pH plate fluorosensor. The sediment cores were taken at a site with pronounced bioturbating and bioirrigating activities in the Gullmar Fjord (northeastern North Sea). (C) High-resolution two-dimensional distributions of pH at the sediment-water interface. The distribution indicated pronounced pH gradients just below the interface, most likely due to the reoxidation of reduced compounds diffusing from below. Visualized are also strong gradients adjacent to burrow structures from macrofaunal (*Nemertea*) reworking. Close to burrow linings there are pronounced drop in pH over relatively short distances, indicating enhanced mineralization of organic matter and reoxidation of reduced metabolites. (D) A close-up of pH distributions adjacent to an abandoned macrofaunal construction, where enhanced bacterial activity close to burrows and fecal aggregates causes a localized decrease in pH.

ganic matter were clearly demonstrated in the intact sediment cores from the Gullmar Fjord (Fig. 6). Pronounced two-dimensional pH gradients were observed at the sediment-water interface, as well as further down in the sediment adjacent to macrofaunal (*Nemertea*) burrows and fecal material. For example, just below the interface, pH decreased about 0.25 pH units over a distance of 4 mm (Fig. 6C). Moreover, an active (visual inspection of worm activity) *Nemertea* burrow had a drop of 1.5 pH units across wall lining sections of approximately 1.1 mm. A pH ~ 6.5 inside the burrow compared to ~8.0 in the bottom water implied substantial acid production (CO₂, HNO₃, H₂SO₄). Heterotrophic and chemoautotrophic bacterial activity is normally enhanced close to sites of redox gradients and reactive organic material such as burrows and fecal aggregates, and presumably drives the observed localized decreases in pH. A close-up of an abandoned worm burrow further supported elevated pH gradients associated with macrofaunal constructions, with or without active macrofauna (Fig. 6D). A large fraction of surface sediment is continually passed through animal guts or incorporated into biogenic structures. The planar optode allows a two-dimensional snapshot of such reaction centers and a method of readily quantifying their importance as a function of time.

Taken in conjunction with two-dimensional O₂ distributions (Glud et al. 1996b, 1998, 1999), the pH fluorosensor should allow strong constraints on conceptualization and quantification of early diagenetic reactions in surface sediments. Eventual future ability to *simultaneously* scan two-dimensional distribution patterns of diagenetically important solutes like oxygen, ΣCO₂, nutrients, calcium, and pH would provide a basis for substantially improved conceptual and quantitative models of early diagenetic reactions, particularly processes related to carbon and nutrient cycling in the complex bioturbated zone of aquatic sediments.

References

- ALLER, R. C. 1982. The effects of macrobenthos on chemical properties of marine sediment and overlying water, p. 53–102. *In* P. L. McCall and M. J. S. Tevesz [eds.], *Animal-sediment relations*. Plenum.
- , AND J. Y. ALLER. 1998. The effect of biogenic irrigation intensity and solute exchange on diagenetic reaction rates in marine sediments. *J. Mar. Res.* **56**: 905–936.
- , P. O. J. HALL, P. D. RUDE, AND J. Y. ALLER. 1998. Biogeochemical heterogeneity and suboxic diagenesis in hemipelagic sediments of the Panama Basin. *Deep-Sea Res.* **45**: 133–165.
- BATES, R. G. 1973. *Determination of pH*. Wiley.
- BISHOP, E. 1972. Theory and principles of visual indicators, p. 13–63. *In* E. Bishop [ed.], *Indicators*. Pergamon.
- BYRNE, R. H., AND J. A. BRELAND. 1989. High precision multi-wavelength pH determinations in seawater using cresol red. *Deep-Sea Res.* **36**: 803–810.
- CAI, W. J., AND C. E. REIMERS. 1993. The development of pH and pCO₂ microelectrodes for studying the carbonate chemistry of pore waters near the sediment-water interface. *Limnol. Oceanogr.* **38**: 1762–1773.
- CARDWELL, T. J., R. W. CATTRALL, L. W. DEADY, M. DORKOS, AND G. R. O'CONNELL. 1993. A fast response membrane-based pH indicator optode. *Talanta* **40**: 765–768.
- DICKSON, A. 1990. Standard potential of the (AgCl + 1/2 H₂ = Ag + HCl) cell and the dissociation constant of bisulfate ion in synthetic sea water from 273.15 to 318.15 K. *J. Chem. Thermodyn.* **22**: 113–127.
- . 1993. The measurements of sea water pH. *Mar. Chem.* **44**: 131–142.
- DYRSSEN, D., AND L. G. SILLÉN. 1967. Alkalinity and total carbonate in sea water. A plea for p-T independent data. *Tellus* **19**: 113–121.
- FROELICH P. N., AND OTHERS. 1979. Early oxidation of organic matter in pelagic sediments of the eastern equatorial Atlantic: Suboxic diagenesis. *Geochim. Cosmochim. Acta* **43**: 1075–1091.
- GLUD, R. N., I. KLIMANT, G. HOLST, O. KOHLS, V. MEYER, M. KUHL, AND J. K. GUNDERSEN. 1999a. Adaptation, test and in-situ measurements with O₂ microopt(r)odes on benthic landers. *Deep-Sea Res.* **46**: 171–183.
- , M. KÜHL, O. KOHLS, AND N. B. RAMSING. 1999b. Heterogeneity of oxygen production and consumption in a photosynthetic microbial mat as studied by planar optodes. *J. Phycol.* **35**: 270–279.
- , N. B. RAMSING, J. K. GUNDERSEN, AND I. KLIMANT. 1996. Planar optodes: A new tool for fine scale measurements of two-dimensional O₂ distribution in benthic communities. *Mar. Ecol. Prog. Ser.* **140**: 217–226.
- , C. M. SANTEGOEDS, D. DE BEER, O. KOHLS, AND N. B. RAMSING. 1998. Oxygen dynamics at the base of a biofilm studied with planar optodes. *Aquat. Microb. Ecol.* **14**: 223–233.
- GRYNKIEWICZ, G., M. POENIE, AND R. Y. TSIEN. 1985. A new generation of Ca²⁺ indicators with greatly improved fluorescence properties. *J. Biol. Chem.* **260**: 3440–3450.
- HANSSON, I. 1973. A new set of pH scales and standard buffers for sea water. *Deep-Sea Res.* **20**: 479–491.
- HARVEY, E. NEWTON. 1957. *A history of luminescence from the earliest times until 1900*. *Memoirs of the American Philosophical Society*, vol. 44. Philadelphia.
- JANATA, J. 1987. Do optical sensors really measure pH? *Anal. Chem.* **59**: 1351–1356.
- KLIMANT, I., V. MEYER, AND M. KÜHL. 1995. Fiber-optic oxygen microsensors, a new tool in aquatic biology. *Limnol. Oceanogr.* **40**: 1159–1165.
- KOSTOV, Y., S. TZONKOV, L. YOTOVA, AND M. KRYSSTOVA. 1993. Membranes for optical pH sensors. *Anal. Chim. Acta* **280**: 15–19.
- LAKOWICZ, J. R. 1999. *Principles of fluorescence spectroscopy*. 2nd ed. Kluwer Academic/Plenum.
- LEINER, M. J. P., AND O. S. WOLFBEIS. 1991. Fiber optic pH sensors, p. 359–384. *In* O. S. Wolfbeis [ed.], *Fiber optic chemical sensors and biosensors*, vol. I. CRC.
- LIN, J. 2000. Recent development and applications of optical and fiber-optic pH sensors. *Trends Anal. Chem.* **19**: 541–552.
- NILSSON, H. C., AND R. ROSENBERG. 2000. Succession in marine benthic habitats and fauna in response to oxygen deficiency: Analysed by sediment profile-imaging and by grab samples. *Mar. Ecol. Prog. Ser.* **197**: 139–149.
- OFFENBACHER, H., O. S. WOLFBEIS, AND E. FÜRLINGER. 1986. Fluorescence optical sensors for continuous determination of near-neutral pH values. *Sensors Actuators* **9**: 73–84.
- PETERSON, J. I., S. R. GOLDSTEIN, R. V. FITZGERALD, AND D. K. BUCKHOLD. 1980. Fiber optic pH probe for physiological use. *Anal. Chem.* **52**: 864–869.
- REIMERS, C. E., K. M. FISCHER, R. MEREWETHER, K. L. SMITH JR., AND R. A. JAHNKE. 1986. Oxygen microprofiles measured *in-situ* in deep ocean sediments. *Nature* **320**: 741–744.
- REVSBECH, N. P. 1989. Diffusion characteristics of microbial com-

- munities determined by the use of oxygen microsensors. *J. Microbiol. Methods* **9**: 111–122.
- , AND B. B. JØRGENSEN. 1986. Microelectrodes: Their use in microbial ecology. *Adv. Microb. Ecol.* **9**: 293–352.
- , ———, AND T. H. BLACKBURN. 1980. Oxygen in the sea bottom measured with a microelectrode. *Science* **207**: 1355–1356.
- RHOADS, D. C., AND J. D. GERMANO. 1982. Characterization of organism-sediment relations using sediment profile imaging: An efficient method of remote ecological monitoring of the seafloor. *Mar. Ecol. Prog. Ser.* **8**: 115–128.
- , J. A. MURAMOTO, C. COYLE, R. H. WARD, R. ANDERSON, G. MOORADIAN, AND J. SUNSHINE. 1994. Hyperspectral UV imaging spectrometer for *in-situ* measurement of organic contamination in bottom sediments. *Mar. Techn. Soc. Conf. Proc., Challenges and Opportunities in the Marine Environment*.
- SAARI, L. A., AND W. R. SEITZ. 1982. pH sensor based on immobilized fluoresceinamine. *Anal. Chem.* **54**: 821–823.
- SEITZ, W. R. 1984. Chemical sensors based on fiber optics. *Anal. Chem.* **56**: 16A–34A.
- SILLÉN, L. G. 1967. Equilibrium concepts in natural water systems. *Adv. Chem. Ser.* **67**. Am. Chem. Soc.
- SMITH, K. L., JR., C. H. CLIFFORD, A. H. ELIASON, B. WALDEN, G. T. ROWE, AND J. M. TEAL. 1976. A free vehicle for measuring benthic community metabolism. *Limnol. Oceanogr.* **21**: 164–170.
- SØRENSEN, S. P. L., AND S. PALITZSCH. 1910. Über die Messung der Wasserstoffionenkonzentration des Meerwassers. *Biochem. Z.* **24**: 387.
- STRÖMBERG, N., AND S. HULTH. 2001. An ammonium selective fluorosensor based on the principles of coextraction. *Anal. Chim. Acta* **443**: 215–225.
- STUMM, W., AND J. J. MORGAN. 1996. *Aquatic chemistry: Chemical equilibria and rates in natural waters*, 3rd ed. Wiley.
- TAKAHASHI, T., R. F. WEISS, C. H. CULBERSON, J. M. EDMOND, D. E. HAMMOND, C. S. WONG, Y.-H. LI, AND A. E. BAINBRIDGE. 1970. A carbonate chemistry profile at the 1969 GEOSECS intercalibration station in the eastern Pacific Ocean. *J. Geophys. Res.* **75**: 7648–7666.
- WERNER, T., AND O. S. WOLFBEIS. 1993. Optical sensor for the pH 10–13 range using new support material. *Freshw. Z. Anal. Chem.* **346**: 564–568.
- WOLFBEIS, O. S. 1985. Acid-base titrations using fluorescent indicators and fiber optical light guides. *Freshw. Z. Anal. Chem.* **320**: 271–271.
- . 1991. *Fiber optical chemical sensors and biosensors*, vol. I and II. CRC.
- , E. FÜRLINGER, H. W. KRONEIS, AND J. H. MARSONER. 1983. A study on fluorescent indicators for near-neutral (“physiological”) pH values. *Freshw. Z. Anal. Chem.* **314**: 119.
- , AND H. OFFENBACHER. 1986. Fluorescence sensor for monitoring ionic strength and physiological pH values. *Sensors Actuators* **9**: 85–91.
- ZHUJUN, Z., AND W. R. SEITZ. 1984. A fluorescence sensor for quantifying pH in the range from 6.5 to 8.5. *Anal. Chim. Acta* **160**: 47–55.

Received: 13 March 2001

Accepted: 30 August 2001

Amended: 2 October 2001